

REGULAR PAPERS

## Reduction in connecting resistivity and optical reflection loss at intermediate layer for mechanically stacked multijunction solar cells

To cite this article: Masahiko Hasumi *et al* 2018 *Jpn. J. Appl. Phys.* **57** 102301

View the [article online](#) for updates and enhancements.



## Reduction in connecting resistivity and optical reflection loss at intermediate layer for mechanically stacked multijunction solar cells

Masahiko Hasumi\*, Yoshihiro Ogawa, Kousuke Oshinari, Jun-ichi Shirakashi, Wakana Kubo, and Toshiyuki Sameshima\*

Department of Electrical and Electronic Engineering, Tokyo University of Agriculture and Technology, Koganei, Tokyo 184-8588, Japan

\*E-mail: mhasumi@cc.tuat.ac.jp; tsamesim@cc.tuat.ac.jp

Received May 16, 2018; accepted July 2, 2018; published online September 5, 2018

Reduction in the connecting resistivity and optical reflection loss at the intermediate region of mechanically stacked multijunction solar cells are discussed. The top and bottom substrates were bonded using an epoxy-type adhesive with dispersed transparent and conductive indium tin oxide (ITO) particles. The connecting resistivity of the intermediate layer was substantially decreased to  $0.12 \Omega \text{cm}^2$  for the stacked Si substrates with 40 nm surfaces roughened by  $\text{SF}_6/\text{Ar}$  plasma irradiation. The optical reflectivity of the stacked GaAs and Si substrates was well decreased by the insertion of 130-nm-thick transparent and conductive indium gallium zinc oxide (IGZO) layers at the interfaces between the semiconductor substrates and the intermediate adhesive. The IGZO layers functioned as antireflection layers and provided high effective absorbance to the bottom Si substrates for light wavelength regions, in which the top GaAs substrate was transparent and the bottom Si substrate was opaque. The effective absorbencies at incident light angles between 0 and  $50^\circ$  ranged from 0.94 to 0.95 for the stacked GaAs and Si structure with IGZO layers, and from 0.80 to 0.82 for the structure without IGZO layers. © 2018 The Japan Society of Applied Physics

### 1. Introduction

Solar cells have widely been investigated as clean energy sources, which produce electrical power directly from sunlight.<sup>1–6</sup> The conversion efficiency  $E_{\text{ff}}$  of a single-junction solar cell depends on the band gap of the semiconductor material.  $E_{\text{ff}}$  is strictly limited at 32.7%, which is called the Shockley–Queisser limitation.<sup>3</sup> To overcome the  $E_{\text{ff}}$  limitation of a single-junction solar cell and realize a higher  $E_{\text{ff}}$ , a multijunction solar cell has been proposed.<sup>7–11</sup> Combinations of solar cells with different band gaps effectively absorb sunlight from the ultraviolet to infrared wavelength regions. Ohmically connected solar cells cooperatively increase the open circuit voltage  $V_{\text{oc}}$ . A three-junction InGaP/GaAs/Ge solar cell with an  $E_{\text{ff}}$  of 31.5% fabricated by the epitaxial crystalline growth method has been reported.<sup>9</sup> Mechanically stacked multijunction solar cells have also been reported.<sup>12–22</sup> The mechanical stacking of individual solar cells allows the use of a wide selection of semiconductor materials such as amorphous, polycrystalline, organic semiconductors, and single-crystalline inorganic semiconductors. Moreover, this method makes it possible to fabricate large solar cells.

We have proposed a method of mechanically stacking semiconductor solar cells with a transparent conductive adhesive with dispersed indium tin oxide (ITO) conductive particles.<sup>23–25</sup> This method is simple and low-cost. However, there are two problems to be solved. First, the connecting resistivity in the adhesive region must be low enough to achieve a high  $E_{\text{ff}}$ . We have already established a process technology with the connecting resistivity lower than  $1.0 \Omega \text{cm}^2$ .<sup>25</sup> It was low enough to fabricate multijunction solar cells with an  $E_{\text{ff}}$  higher than 30%. However, to fabricate solar cells with an  $E_{\text{ff}}$  reaching 40% and higher, for example, concentrating-type solar cells, further decrease in connecting resistivity is required. The second problem is optical reflection loss in the intermediate adhesive interface region. Semiconductor materials have high reflective indexes in general because of their strong covalent bonding, while an organic adhesive has a low refractive index. This difference in the refractive index causes high optical reflection, which reduces

the transmittance of light into the bottom cell. Optical reflection should be reduced to maintain the current matching condition between the top and bottom cells, which is an important condition to achieve a high  $E_{\text{ff}}$ . We propose the formation of transparent and conductive indium gallium zinc oxide (IGZO) layers at the interfaces between the semiconductor substrates and intermediate adhesive to reduce optical reflection loss.<sup>26–28</sup> IGZO layers have the antireflection effect because the refractive index of IGZO of 1.85 is lower than those of semiconductor materials and higher than that of an epoxy adhesive. We previously reported the decrease in the optical reflectivity of mechanically stacked samples with IGZO layers for normal light incidence.<sup>27</sup> Since the angle of incident sunlight changes with time in a day and with the season, the investigation of reduction in optical reflectivity at different incident light angles is required.

In this paper, we report the experimental demonstration of the reduction in the connecting resistivity and optical reflection loss at different incident light angles. The connecting resistivity of the intermediate layer between the stacked substrates with rough surfaces is well decreased.  $\text{SF}_6/\text{Ar}$  plasma irradiation roughens the surfaces of the Si substrates and reduces the connecting resistivity by improving the electrical contact between ITO particles and the substrates. We also use stacked top GaAs and bottom Si samples to examine their optical reflectivity properties of different incident light angles. Two transparent and conductive IGZO layers are inserted into the bottom surface of the top GaAs substrate and the top surface of the bottom Si substrate. We report the experimental demonstration of the effective reduction in optical reflection loss with incident angle. In addition, we discuss the effective optical absorbance  $A_{\text{eff}}$  of the bottom substrate. We demonstrate that high  $A_{\text{eff}}$  values were maintained at incident angles ranging from 0 to  $50^\circ$  by the insertion of IGZO antireflection layers.

### 2. Experimental methods

4-in.-sized n-type (100) Si substrates polished on both surfaces with a thickness of  $500 \mu\text{m}$  and a resistivity of  $0.001 \Omega \text{cm}$  were prepared to investigate the connecting resistivity of

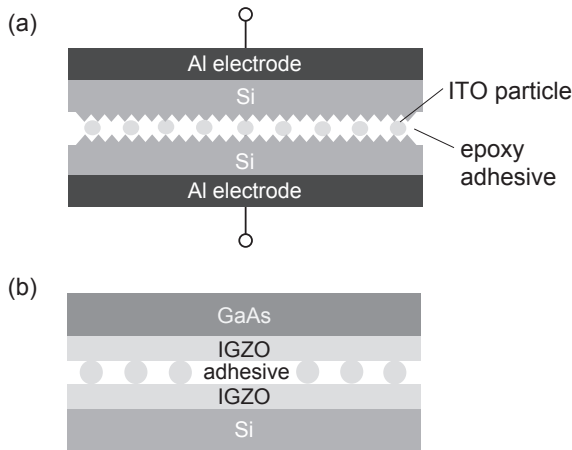


**Fig. 1.** Schematic images of sample structures. (a) Sample with stacked top and bottom Si substrates with rough surfaces. (b) Stacked top GaAs and bottom Si substrates with IGZO antireflection layers.

samples with stacked structures. The top surface of the substrates was irradiated with 13.56 MHz radio-frequency SF<sub>6</sub>/Ar plasma at a power of 200 W and a gas pressure of 1.7 Pa for a duration range from 4 to 40 min at room temperature. The gas flow rates of SF<sub>6</sub> and Ar were 5 and 10 sccm, respectively. The SF<sub>6</sub> residue was removed with hydrofluoric acid. Then, the substrates were cut into 2 × 2 cm<sup>2</sup> pieces. The surface roughness was investigated by atomic force microscopy (AFM). An Al electrode was formed on the rear surface of the pieces by vacuum evaporation. Then, the samples with a structure shown in Fig. 1(a) were formed by mechanical stacking. A transparent and conductive adhesive was prepared by dispersing 6 wt % (1 vol %) 20-μm-diameter ITO particles in an epoxy-type adhesive. Then, it was applied on the rough surfaces of the bottom Si pieces. The top pieces were placed on the adhesive such that the rough surfaces were face-to-face. The stacked pieces were kept for 2 h at room temperature in 0.8 MPa nitrogen gas atmosphere to solidify the adhesive. We also fabricated samples with stacked as-polished Si substrates under the same stacking conditions except for the surface roughness. The thickness of the adhesive layer was about 20 μm for both rough- and polished-surface stacked samples. The current–voltage characteristics of the samples were measured using a conventional source meter. The change in the connecting resistivity of the samples kept in an environment with a temperature of 20 °C and a humidity of 50% for 2500 h was also measured.

To fabricate samples of stacked GaAs and Si substrates with IGZO antireflection layers as shown in Fig. 1(b), we prepared 500-μm-thick n-type 17 Ω cm (100) Si and 500-μm-thick n-type 20 Ω cm (100) GaAs substrates. Our optical investigation focused on the wavelength region, in which the top GaAs substrate is transparent and the bottom Si substrate is opaque. The measurement of optical reflectivity spectra determined the wavelength region with the shortest wavelength λ<sub>1</sub> as 902 nm and the longest wavelength λ<sub>2</sub> as 1020 nm. 130-nm-thick IGZO films were formed on the bottom surface of GaAs and the top surface of the Si substrate by radio-frequency Ar plasma sputtering at 2000 W with In<sub>1.0</sub>Ga<sub>1.2</sub>Zn<sub>1.0</sub>O<sub>1.4</sub> as the target at room temperature. The films were designed to reduce the optical reflection loss at wavelengths between λ<sub>1</sub> and λ<sub>2</sub> using a calculation program

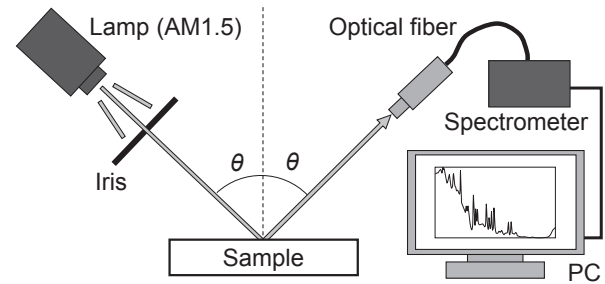


**Fig. 2.** Schematic image of home-made optical reflection measurement system with incident angle from 10 to 50°.

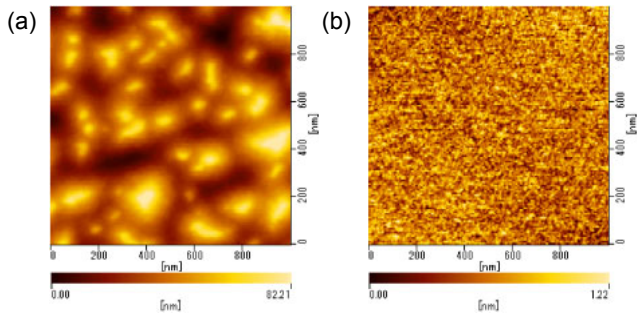
to be discussed in Sect. 3.3. The IGZO layers formed on the semiconductor surfaces were heated at 350 °C in air atmosphere for 1 h to increase the resistivity to 0.056 Ω cm to prevent serious free-carrier absorption in the infrared wavelength region. The increase in connecting resistivity caused by the insertion of IGZO anti-reflection layers was negligible because of the low resistivity and small thickness of the layers. The adhesive with ITO particles was applied on the IGZO surface of the bottom Si substrate. The top GaAs substrate was placed on the adhesive such that the IGZO surfaces were face-to-face. The epoxy adhesive was then solidified. A sample was thus fabricated with the structure of stacked GaAs/130-nm-thick IGZO/adhesive/130-nm-thick IGZO/Si. Moreover, another sample with the structure of stacked GaAs/adhesive/Si was also fabricated as a control. Optical reflectivity spectra of the samples were measured from 500 to 2000 nm with normal incidence using a conventional spectrometer. A homemade optical reflection measurement system shown in Fig. 2 was also constructed to investigate the optical reflection properties at various incident light angles. Slanting light of AM 1.5 was irradiated on the top GaAs surface of the samples. The reflection light spectra at wavelengths ranging from 650 to 1050 nm were measured using an optical-fiber coupled spectrometer. The angles of incident and reflectance lights, θ, were coincidentally changed from 10 to 50°. The iris was set on the incident light path to prevent stray light. The reflectivity spectra were calibrated using samples of the Al mirror and Si substrates.

### 3. Results and discussion

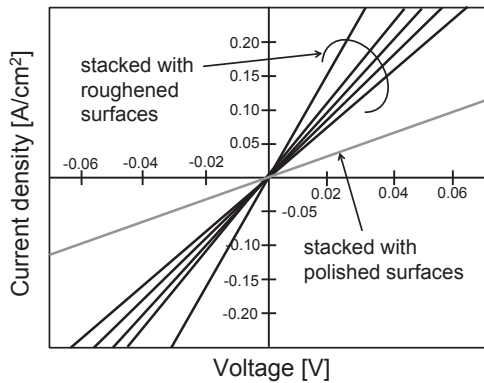
#### 3.1 Reduction in connecting resistivity

Figure 3 shows AFM images of the 16-min SF<sub>6</sub>/Ar plasma-irradiated (a) and as-polished (b) surfaces of crystalline Si substrates. The plasma irradiation resulted in the rough-textured structure on the surface. The maximum height roughness  $R_z$  between the peak and the valley of 64 nm and the root mean square roughness  $R_{RMS}$  of 34 nm were obtained from the image of the sample with 16 min plasma irradiation.  $R_{RMS}$  gradually increased to 40 nm as the plasma irradiation duration increased to 40 min. On the other hand, no surface structure was observed on the as-polished surface of crystalline Si substrates.  $R_{RMS}$  was less than 0.2 nm. These results clearly indicate that the rough-textured structure was successfully formed on the Si surface by the plasma treatment.

Figure 4 shows the current voltage characteristics of the samples of stacked Si substrates. The black lines indicate the samples of stacked substrates with roughened surfaces, as shown in Fig. 1(a), and the gray line indicates the sample of



**Fig. 3.** (Color online) AFM images of SF<sub>6</sub>/Ar-plasma-irradiated (a) and as-polished (b) surfaces of Si substrates.



**Fig. 4.** Current voltage characteristics of the stacked Si substrates. The black lines indicate the samples stacked with roughened surfaces, as shown in Fig. 1(a), and the gray line indicates the sample stacked with polished surfaces for comparison.

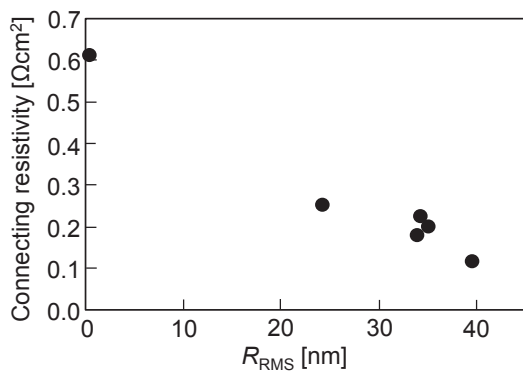


**Fig. 5.** Connecting resistivity of the stacked Si substrates as a function of  $R_{\text{RMS}}$ .

stacked substrates with polished surfaces for comparison. Both the rough- and polished-surface stacking samples showed ohmic current voltage characteristics. The connecting resistivities of the samples stacked with rough surfaces ranged from 0.12 to 0.27  $\Omega\text{cm}^2$ . On the other hand, the connecting resistivity of the sample stacked with polished surfaces was 0.61  $\Omega\text{cm}^2$ . Although the mechanical stacking conditions were the same, all the samples stacked with rough surfaces showed lower connecting resistivities than the sample stacked with polished surfaces. Figure 5 shows the connecting resistivity of the samples of stacked Si substrates as a function of  $R_{\text{RMS}}$ . The connecting resistivity gradually decreased as  $R_{\text{RMS}}$  increased. The lowest connecting resist-

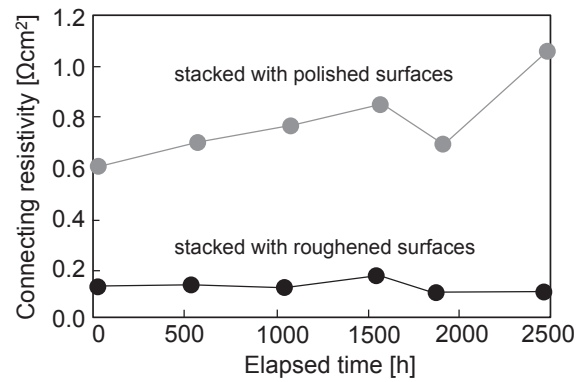


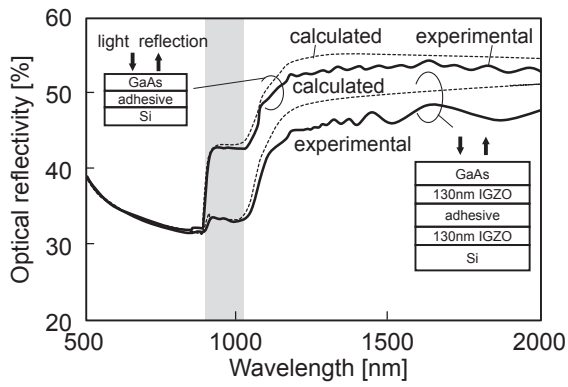
**Fig. 6.** Connecting resistivity of the stacked Si substrates as a function of elapsed time.

ivity of 0.12  $\Omega\text{cm}^2$  was obtained for the sample stacked with an  $R_{\text{RMS}}$  of 40 nm treated with the SF<sub>6</sub>/Ar plasma irradiation for 40 min. The electrical connection between the top and bottom Si substrates was formed by the 20- $\mu\text{m}$ -diameter ITO particles dispersed in the adhesive. The 40 nm roughness was almost negligible compared with the size of ITO particles and the thickness (20  $\mu\text{m}$ ) of the adhesive region. We believe that the 1.8-fold increase in the surface area, as indicated by the AFM measurement, decreased the contact resistivity between ITO particles and the surface of Si substrates. The surface roughness of the Si substrates increases the contact area between ITO particles and the substrates, and it may increase the number of ITO particles contributing to the electrical connection formed between the top and bottom Si substrates.

Figure 6 shows the connecting resistivity of the sample stacked with an  $R_{\text{RMS}}$  of 40 nm and the sample stacked with the polished surfaces as a function of elapsed time. The connecting resistivity of the sample stacked with polished surfaces gradually increased with time and became 1.05  $\Omega\text{cm}^2$  after 2500 h. We assume that the increase in connecting resistivity was caused by the decrease in the number of ITO particles contributing to the electrical connection due to a slight volume change of the adhesive caused by moisture absorption. This becomes a serious problem because the increase in connecting resistivity directly leads to the decrease in the conversion efficiency of multijunction solar cells. Although this may be solved using an appropriate sealing technology for modularization, we have found a way to keep the connecting resistivity low. The connecting resistivity of the sample stacked with rough surfaces hardly changed and remained low for 2500 h. There is a possibility that the mechanical strength of adhesion was improved, in addition to the decrease in the connecting resistivity, owing to the rough surface of the Si substrates. These results are only preliminary, but we have shown the improvement of electrical contacts between ITO particles and the roughened surfaces of Si substrates. Since the reliability of epoxy resin is uncertain, tests of this adhesive layer in hot and high humidity environments are required. Other adhesives with high environmental resistance such as polyimide may also be selected.<sup>21)</sup>

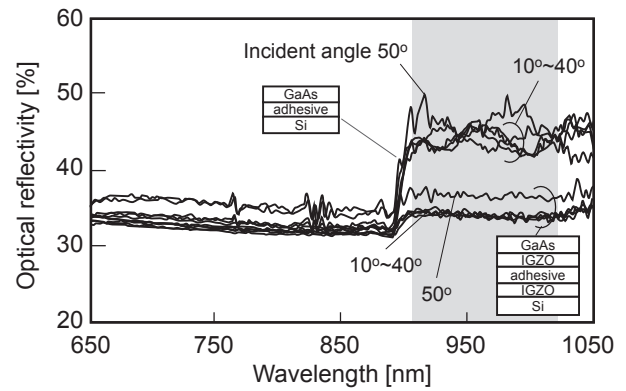
### 3.2 Reduction in optical reflection loss

Figure 7 shows the optical reflectivity spectra of the samples with the structures of stacked GaAs/130-nm-thick IGZO/adhesive/130-nm-thick IGZO/Si and GaAs/adhesive/Si at normal incidence obtained from our previous report.<sup>27)</sup> The



**Fig. 7.** Experimental and calculated optical reflectivity spectra of the samples with structures of stacked GaAs/130-nm-thick IGZO/adhesive/130-nm-thick IGZO/Si and GaAs/adhesive/Si with normal incident.<sup>27)</sup> The hatched area shows the wavelength region in which the top GaAs substrate is transparent and the bottom Si substrate is opaque.

hatched area shows the wavelength region ranging from  $\lambda_1$  to  $\lambda_2$ , where the top GaAs substrate is transparent and the bottom Si substrate is opaque. When the wavelength is shorter than  $\lambda_1$ , the top GaAs substrate is opaque. The optical reflectivity of samples is determined by the reflectivity of the interface between air and the GaAs substrate. Therefore, the reflectivity spectra of both samples were the same. On the other hand, when the wavelength is located between  $\lambda_1$  and  $\lambda_2$ , the top GaAs substrate becomes transparent. Light coming into the top surface is partially reflected in the intermediate adhesive region and returns to the top surface because the bottom Si substrate is still opaque. The optical reflectivity measurement at the top surface therefore gives the degree of optical reflection in the intermediate adhesive region. The sample with the structure of stacked GaAs/130-nm-thick IGZO/adhesive/130-nm-thick IGZO/Si showed optical reflectivities ranging from 33 to 34% in the hatched wavelength region. On the other hand, the control sample with the structure of stacked GaAs/adhesive/Si, showed high optical reflectivities between 40 and 42% in the hatched region. The low optical reflectivities clearly demonstrated the antireflection effect of the IGZO layer. When the wavelength is longer than  $\lambda_2$ , the bottom Si substrate becomes transparent and multiple reflections among all the interfaces contribute to the optical reflectivity of the sample. Therefore, the optical reflectivity further increased for both stacked samples, as shown in Fig. 7. Figure 7 also shows the calculated optical reflectivity spectra (dashed curves) of the samples with structures of stacked GaAs/130-nm-thick IGZO/adhesive/130-nm-thick IGZO/Si and GaAs/adhesive/Si. The Fresnel-type optical interference effect was calculated for the IGZO layers, assuming a simple plain wave model.<sup>29–31)</sup> The calculated optical reflectivity spectra were in good agreement with the experimental spectra of the samples with the structures of stacked GaAs/130-nm-thick IGZO/adhesive/130-nm-thick IGZO/Si and GaAs/adhesive/Si. This good agreement among experimental and calculated values in the hatched region indicates that the optical reflectivity was due to the effect of multiple reflections among the top surface of crystalline GaAs, the optical-phase-coupled interface of IGZO/adhesive and GaAs, and the interface of IGZO/adhesive and Si.



**Fig. 8.** Experimental optical reflectivity spectra of the samples with structures of stacked GaAs/130-nm-thick IGZO/adhesive/130-nm-thick IGZO/Si and GaAs/adhesive/Si with incident angles ranging from 10 to 50° measured using the system shown in Fig. 2.

Figure 8 shows the optical reflectivity spectra of the samples with structures of stacked GaAs/130-nm-thick IGZO/adhesive/130-nm-thick IGZO/Si and GaAs/adhesive/Si with incident angles ranging from 10 to 50° measured using the system shown in Fig. 2. The hatched area also shows the wavelength region ranging from  $\lambda_1$  to  $\lambda_2$ . When the wavelength is shorter than  $\lambda_1$ , the optical reflectivity of samples is determined by the reflectivity of the interface between air and the GaAs substrate. The optical reflectivity spectra of both samples are the same at each incident angle. On the other hand, when the wavelength is located between  $\lambda_1$  and  $\lambda_2$ , the top GaAs substrate becomes transparent. In the cases of incident angles ranging from 10 to 40°, the sample with 130-nm-thick IGZO layers formed on the bottom surface of the GaAs substrate and the top surface of the Si substrate showed almost the same optical reflectivity spectra. The reflectivities ranged from 33 to 35% in the hatched wavelength region. In the case of an incident angle of 50°, slightly high reflectivities ranging from 36 to 38% were obtained. These low optical reflectivities clearly demonstrate that the IGZO layer showed the antireflection effect. Light was effectively transmitted from GaAs to Si without substantial light reflection in the intermediate adhesive region. On the other hand, the control sample with the structure of stacked GaAs/adhesive/Si, showed high optical reflectivities ranging from 42 to 50% in the hatched region at incident angles ranging from 10 to 50°. These high optical reflectivities were due to substantial optical reflection at the interfaces between GaAs and the adhesive, and between the adhesive and Si. These results were consistent with the optical reflectivity behavior shown in Fig. 7 measured using a conventional spectrometer.

### 3.3 Effective optical absorbance

To estimate the optical reflection loss in the intermediate adhesive region, we defined the effective optical absorbance of the bottom cell,  $A_{\text{eff}}$ , as

$$A_{\text{eff}} = \frac{\int_{\lambda_1}^{\lambda_2} [100 - R_s(\lambda)] d\lambda}{\int_{\lambda_1}^{\lambda_2} [100 - r(\lambda)] d\lambda}, \quad (1)$$

where  $R_s(\lambda)$  is the optical reflectivity (%) of the sample at the wavelength  $\lambda$ , and  $r(\lambda)$  is the reflectivity (%) at the top surface

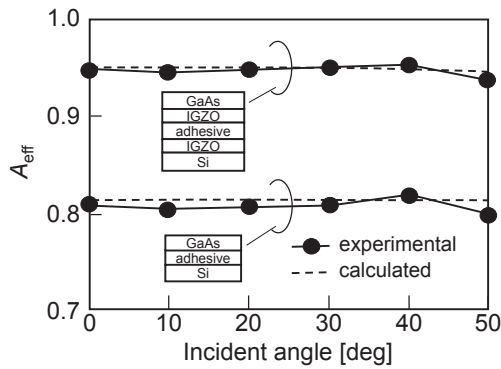


**Fig. 9.**  $A_{\text{eff}}$  as a function of incident angle for the samples with structures of stacked GaAs/130-nm-thick IGZO/adhesive/130-nm-thick IGZO/Si and GaAs/adhesive/Si.

of a GaAs substrate. The denominator of Eq. (1) is the integration of light incidence ratio into the top GaAs substrate between  $\lambda_1$  and  $\lambda_2$  because the GaAs substrate was transparent between  $\lambda_1$  and  $\lambda_2$ . The values of the denominator at each incident angle were experimentally obtained from the reflectivity spectra of GaAs substrate. The numerator is the integration of the optical absorption ratio of the sample between  $\lambda_1$  and  $\lambda_2$ . Because the bottom Si substrate was opaque at wavelengths shorter than  $\lambda_2$ , the numerator of Eq. (1) depends on the optical reflectivity at the interface adhesive layer. Therefore,  $A_{\text{eff}}$  gives the effective optical absorbance of the bottom Si substrate for the light incident on the top GaAs substrate. The optical reflection loss ratio of the intermediate adhesive layer between  $\lambda_1$  and  $\lambda_2$  is therefore given by  $1 - A_{\text{eff}}$ . Figure 9 shows  $A_{\text{eff}}$  as a function of the incident angle  $\theta$  for the samples with the structures of stacked GaAs/130-nm-thick IGZO/adhesive/130-nm-thick IGZO/Si and GaAs/adhesive/Si experimentally obtained from the results of Figs. 7 and 8. High  $A_{\text{eff}}$  values ranging from 0.94 to 0.95 with  $\theta$  values ranging from 0 to 50° were obtained for the sample with the structure of stacked GaAs/130-nm-thick IGZO/adhesive/130-nm-thick IGZO/Si. On the other hand, the  $A_{\text{eff}}$  values of the sample of stacked GaAs/adhesive/Si ranged from 0.80 to 0.82.

We have already reported the calculated  $A_{\text{eff}}$  values with normal incidence for the mechanically stacked samples with IGZO layers. Details of the calculation are also described in our previous report.<sup>27)</sup> The solid curve shown in Fig. 10 represents the calculated  $A_{\text{eff}}$  with an incident angle of 0° for the GaAs and Si stacked sample as a function of the thickness of IGZO antireflection layers.  $A_{\text{eff}}$  increased as the IGZO layer thickness increased and peaked at 130 nm. The maximum  $A_{\text{eff}}$  was 0.95.  $A_{\text{eff}}$  gradually decreased as the IGZO thickness further increased after reaching the peak because the antireflection condition shifted to longer wavelengths. The zero thickness of IGZO indicated the control sample, which gave the lowest  $A_{\text{eff}}$  of 0.81. The control sample showed the highest optical reflection loss at the intermediate adhesive layer. The best effective antireflection wavelength  $\lambda_{\text{eff}}$  of an incident plain wave of light with normal incidence is given by

$$\lambda_{\text{eff}} = 4nd, \tag{2}$$

where  $n$  and  $d$  are the refractive index and the thickness of the antireflection layer. In the present case,  $n$  and  $d$  were 1.85 and

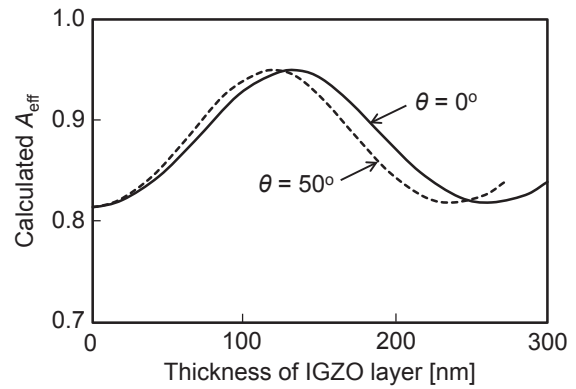


**Fig. 10.** Calculated  $A_{\text{eff}}$  of GaAs and Si stacked sample as a function of thickness of IGZO antireflection layers with incident angles of 0 and 50°.

130 nm, respectively. An  $\lambda_{\text{eff}}$  of 962 nm was located almost at the midpoint between  $\lambda_1$  (902 nm) and  $\lambda_2$  (1020 nm). Therefore, it is natural to obtain a high  $A_{\text{eff}}$  at  $\theta$  of 0°. However, the effective optical path length of the IGZO layer was changed by the incident angle. Since the refractive index of IGZO is large (1.85), the effective incident angle in the IGZO layer is smaller than  $\theta$  at the top surface of the sample in air, as shown in Fig. 2. When the  $\theta$  of the top GaAs surface increased from 0 to 50°, the effective incident angle in the IGZO layer increased from 0 to 24° and the effective optical thickness of the IGZO layer decreased to 118 nm. Therefore,  $A_{\text{eff}}$  peaked at 118 nm and  $A_{\text{eff}}$  at the IGZO thickness of 130 nm slightly decreased to 0.94 at  $\theta$  of 50°, as shown by dashed curve in Fig. 10. The change in  $A_{\text{eff}}$  with the change in  $\theta$  was small and  $A_{\text{eff}}$  remained high.

The calculated  $A_{\text{eff}}$  values are also indicated by dashed lines in Fig. 9. The calculated  $A_{\text{eff}}$  of the structure of stacked GaAs/130-nm-thick IGZO/adhesive/130-nm-thick IGZO/Si slightly decreased from 0.95 to 0.94 as  $\theta$  increased from 0 to 50°. On the other hand, the calculated  $A_{\text{eff}}$  of the structure of stacked GaAs/adhesive/Si was 0.81. It does not change with the incident angle because there are no IGZO interference layers. The calculated  $A_{\text{eff}}$  showed good agreement with the experimentally obtained values, as shown in Fig. 9. Although it was only a simple geometric calculation, it explained the experimental results. High  $A_{\text{eff}}$  values can simply be achieved by forming single-layered antireflection IGZO films with appropriate thicknesses.

#### 4. Conclusions

We demonstrated the reduction in connecting resistivity and optical reflection loss in the intermediate region of mechanically stacked samples bonded with the ITO particles dispersed in epoxy-type adhesive. The roughening of surfaces of the Si substrates by SF<sub>6</sub>/Ar plasma irradiation at 200 W formed a good electrical contact between ITO particles and substrates. The connecting resistivity of the intermediate layer was substantially decreased to 0.12 Ω cm<sup>2</sup> for the sample of stacked Si substrates with  $R_{\text{RMS}}$  of 40 nm. The reduction in optical reflection loss was achieved owing to the IGZO antireflection layers with a refractive index of 1.85 at the intermediate adhesive layer for mechanically stacked samples. Two kinds of stacked samples with the structures of stacked GaAs/130-nm-thick IGZO/adhesive/130-nm-thick IGZO/Si and GaAs/adhesive/Si were fabri-

cated using 6 wt % 20- $\mu\text{m}$ -diameter ITO particles dispersed in the epoxy-type adhesive with a refractive index of 1.47. At incident angles ranging from 0 to 50°, the sample with structure of stacked GaAs/130-nm-thick IGZO/adhesive/130-nm-thick IGZO/Si showed low optical reflectivities ranging from 33 to 35% in the wavelength region ranging from  $\lambda_1$  (902 nm) to  $\lambda_2$  (1020 nm), where the top GaAs substrate is transparent and the bottom Si substrate is opaque. These values were lower than the optical reflectivities of a simple stacked sample without IGZO layers. These experimental results demonstrated that the IGZO layer has the antireflection effect at the intermediate adhesive region at various incident angles. Numerical analysis of the optical reflectivity spectra gave the best IGZO thickness of 130 nm for the highest effective absorbance  $A_{\text{eff}}$ . The samples stacked with the IGZO antireflection layers described above successfully gave high  $A_{\text{eff}}$  values ranging from 0.94 to 0.95 with incident angles ranging from 0 to 50°, while the sample without IGZO layers gave  $A_{\text{eff}}$  values ranging from 0.80 to 0.82 only.

### Acknowledgments

This work was supported by the New Energy and Industrial Technology Development Organization (NEDO) and Sameken Co., Ltd.

- 1) M. A. Green, *Nat. Energy* **1**, 15015 (2016).
- 2) M. A. Green, K. Emery, Y. Hishikawa, W. Warta, and E. D. Dunlop, *Prog. Photovoltaics* **24**, 3 (2016).
- 3) W. Shockley and H. J. Queisser, *J. Appl. Phys.* **32**, 510 (1961).
- 4) J. Zhao, A. Wang, M. A. Green, and F. Ferrazza, *Appl. Phys. Lett.* **73**, 1991 (1998).
- 5) A. Shah, H. Schade, M. Vanecek, J. Meier, E. Vallat-Sauvain, N. Wyrsh, U. Kroll, C. Droz, and J. Bailat, *Prog. Photovoltaics* **12**, 113 (2004).
- 6) K. Yoshikawa, H. Kawasaki, W. Yoshida, T. Irie, K. Konishi, K. Nakano, T. Uto, D. Adachi, M. Kanematsu, H. Uzu, and K. Yamamoto, *Nat. Energy* **2**, 17032 (2017).
- 7) H. Sugiura, C. Amano, A. Yamamoto, and M. Yamaguchi, *Jpn. J. Appl. Phys.* **27**, 269 (1988).
- 8) J. M. Olson, S. R. Kurtz, A. E. Kibbler, and P. Faine, *Appl. Phys. Lett.* **56**, 623 (1990).
- 9) T. Takamoto, M. Kaneiwa, M. Imaizumi, and M. Yamaguchi, *Prog. Photovoltaics* **13**, 495 (2005).
- 10) R. R. King, D. C. Law, K. M. Edmondson, C. M. Fetzer, G. S. Kinsey, H. Yoon, R. A. Sherif, and N. H. Karam, *Appl. Phys. Lett.* **90**, 183516 (2007).
- 11) D. Shahrjardi, S. W. Bedell, C. Ebert, C. Bayram, B. Hekmatshoar, K. Fogel, P. Lauro, M. Gaynes, T. Gokmen, J. A. Ott, and D. K. Sadana, *Appl. Phys. Lett.* **100**, 053901 (2012).
- 12) H. Mizuno, K. Makita, and K. Matsubara, *Appl. Phys. Lett.* **101**, 191111 (2012).
- 13) H. Mizuno, K. Makita, T. Sugaya, R. Oshima, Y. Hozumi, H. Takato, and K. Matsubara, *Jpn. J. Appl. Phys.* **55**, 025001 (2016).
- 14) H. Mizuno, K. Makita, T. Tayagaki, T. Mochizuki, T. Sugaya, and H. Takato, *Appl. Phys. Express* **10**, 072301 (2017).
- 15) S. Essig, C. Allebe, T. Remo, J. F. Geisz, M. A. Steiner, K. Horowitz, L. Barraud, J. S. Ward, M. Schnabel, A. Descoedres, D. L. Young, M. Woodhouse, M. Despeisse, C. Ballif, and A. Tamboli, *Nat. Energy* **2**, 17144 (2017).
- 16) M. A. Steiner, J. F. Geisz, J. S. Ward, I. García, D. J. Friedman, R. R. King, P. T. Chiu, R. M. France, A. Duda, W. J. Olavarria, M. Young, and S. R. Kurtz, *IEEE J. Photovoltaics* **6**, 358 (2016).
- 17) R. Cariou, J. Benick, P. Beutel, N. Razek, C. Flotgen, M. Hermle, D. Lackner, S. W. Glunz, A. W. Bett, M. Wimplinger, and F. Dimroth, *IEEE J. Photovoltaics* **7**, 367 (2017).
- 18) T. Ameri, G. Dennler, C. Lungenschmied, and C. J. Brabec, *Energy Environ. Sci.* **2**, 347 (2009).
- 19) S. Wenger, S. Seyrling, A. N. Tiwari, and M. Grätzel, *Appl. Phys. Lett.* **94**, 173508 (2009).
- 20) N. Shigekawa, J. Liang, R. Onitsuka, T. Agui, H. Juso, and T. Takamoto, *Jpn. J. Appl. Phys.* **54**, 08KE03 (2015).
- 21) T. Sameshima, J. Takenezawa, M. Hasumi, T. Koida, T. Kaneko, M. Karasawa, and M. Kondo, *Jpn. J. Appl. Phys.* **50**, 052301 (2011).
- 22) T. Sameshima, H. Nomura, S. Yoshidomi, and M. Hasumi, *Jpn. J. Appl. Phys.* **53**, 05FV07 (2014).
- 23) S. Yoshidomi, M. Hasumi, T. Sameshima, K. Makita, K. Matsubara, and M. Kondo, Proc. 6th Thin Film Materials and Devices Meet., 2012, 130222027.
- 24) S. Yoshidomi, J. Furukawa, M. Hasumi, and T. Sameshima, *Energy Procedia* **60**, 116 (2014).
- 25) S. Yoshidomi, M. Hasumi, and T. Sameshima, *Appl. Phys. A* **116**, 2113 (2014).
- 26) S. Yoshidomi, S. Kimura, M. Hasumi, and T. Sameshima, *Jpn. J. Appl. Phys.* **54**, 112301 (2015).
- 27) T. Sameshima, T. Nimura, T. Sugawara, Y. Ogawa, S. Yoshidomi, S. Kimura, and M. Hasumi, *Jpn. J. Appl. Phys.* **56**, 012602 (2017).
- 28) M. Hasumi, Y. Ogawa, K. Oshinari, and T. Sameshima, Ext. Abstr. Solid State Devices and Materials, 2017, p. 139.
- 29) E. D. Palik, *Handbook of Optical Constants of Solids* (Academic Press, Orlando, FL, 1985) Subpart 2.
- 30) M. Born and E. Wolf, *Principles of Optics* (Pergamon, New York, 1974) Chaps. 1 and 13.
- 31) K. Ukawa, Y. Kanda, T. Sameshima, N. Sano, M. Naito, and N. Hamamoto, *Jpn. J. Appl. Phys.* **49**, 076503 (2010).